SUPPORTING INFORMATION

Section 1: Supporting information figures

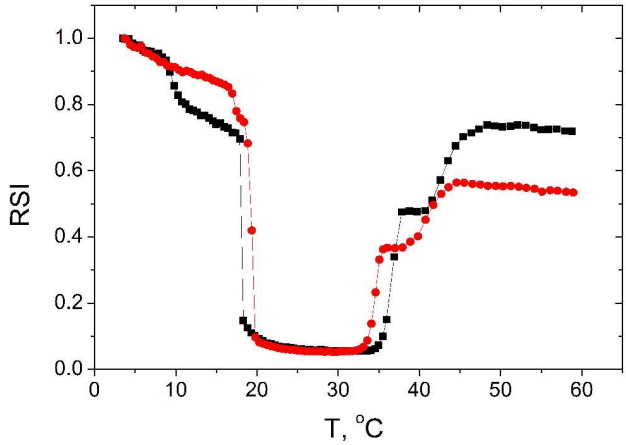

Supporting information figure 1. Examples of individual relative scattering scans. Scans for pure DMPG (black) and DMPG:CHOL=95.2:4.8 (red) are shown, in both DMPG=1 mM.

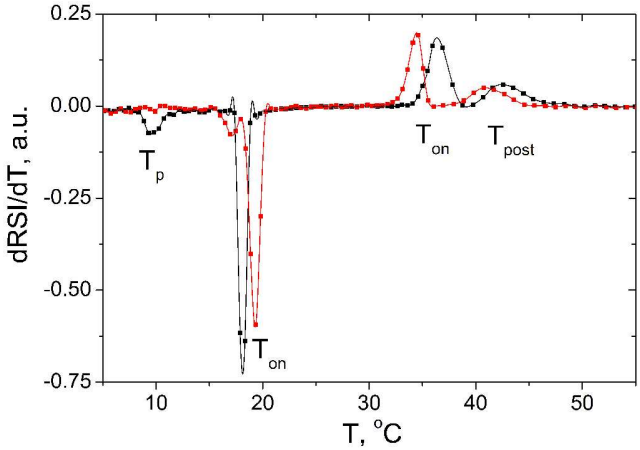

Supporting information figure 2. Example of the analysis of the numerical temperature derivatives of the scattering intensity data. The calculated values for the derivatives are shown as squares for heating scans of pure DMPG (black) and DMPG:CHOL=95.2:4.8 (red). The continuous lines are the results of spline interpolation that was used to determine the temperatures of the peaks.

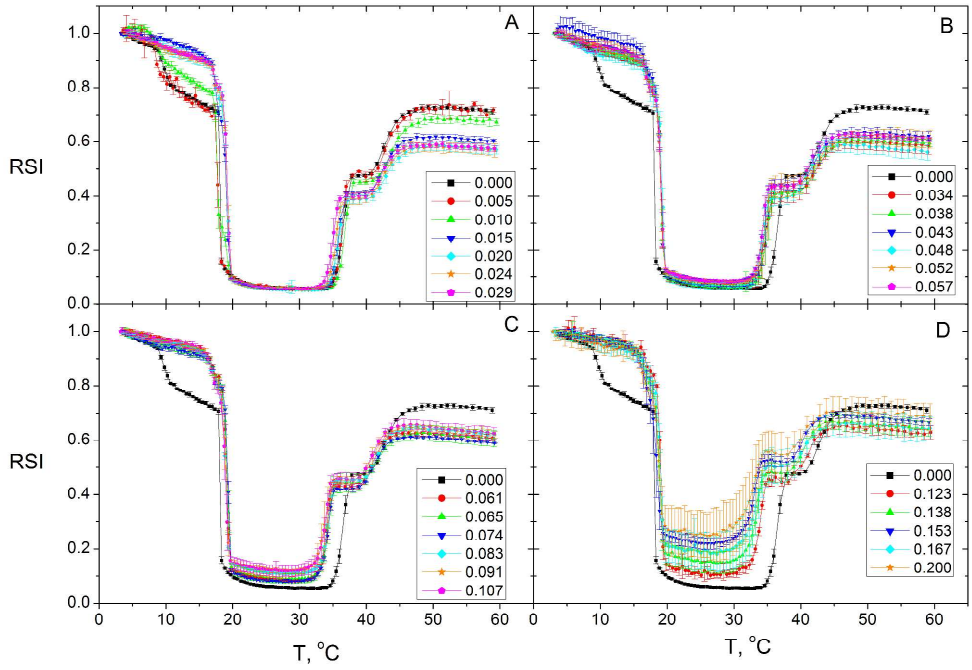

Supporting information figure 3. The relative 90° scattering intensity vs. temperature scans for cholesterol-containing 1 mM DMPG samples. The scattering intensity was normalized with respect to first temperature. The numbers shown in graph next to symbols indicate the cholesterol mole fractions. Pure DMPG is shown in all panels for comparison.

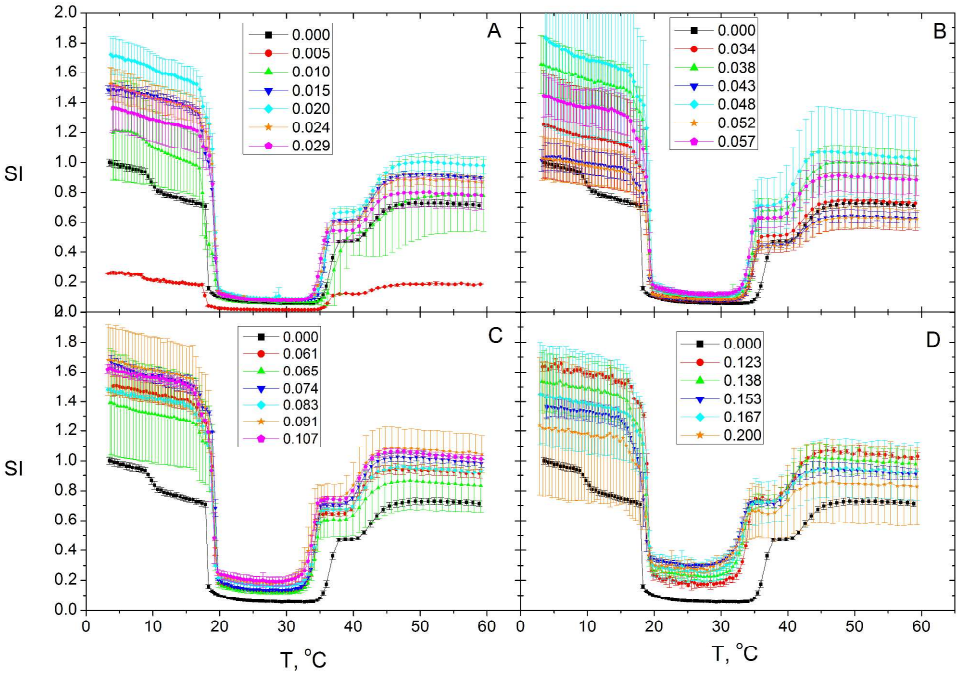

Supporting information figure 4. The relative 90° scattering intensity vs. temperature scans for cholesterol-containing 1 mM DMPG samples. The scattering intensity was normalized with respect to the average scattering intensity of pure DMPG samples at the lowest temperature. The numbers shown in graph next to symbols indicate the cholesterol mole fractions. Pure DMPG is shown in all panels for comparison.

Deleted: <sp>

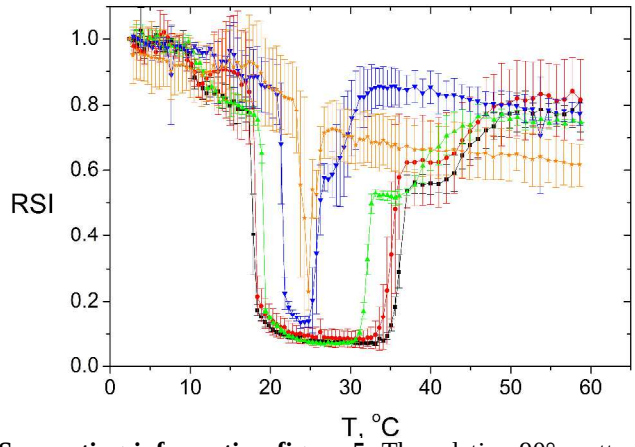

Supporting information figure 5. The relative 90° scattering intensity vs. temperature scans for DMSO-containing 1 mM DMPG samples. The scattering intensity was normalized with respect to first temperature of each curve. The black squares are the data in the absence of DMSO, and the red circles, green up triangles, blue down triangles, and orange stars represent data for DMSO = 1, 5, 15, and 25 vol%, respectively.

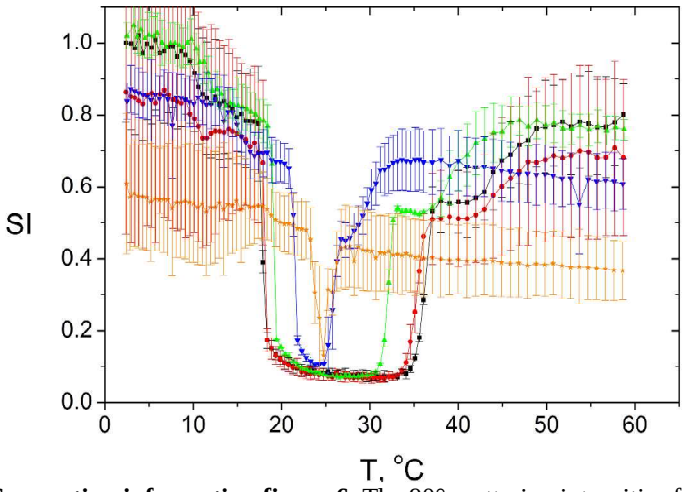

Supporting information figure 6. The 90° scattering intensities for DMPG vesicles in the presence of DMSO. The black squares are the data in the absence of DMSO, and the red circles, green up triangles, blue down triangles, and orange stars represent data for DMSO = 1, 5, 15, and 25 vol%, respectively. The scattering intensity was normalized with respect to the average scattering intensity of pure DMPG samples at the lowest temperature.

Deleted: <sp>¶

Formatted: Font color: Black

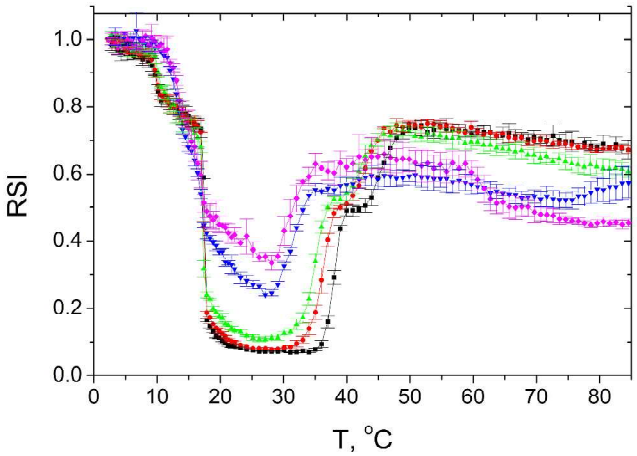

Supporting information figure 7. The relative 90° scattering intensities for DMG-containing DMPG vesicles as a function of temperature. The black squares, red circles, green up triangles, blue down triangles, and magenta diamonds represent data for X_{DMG} = 0, 0.005, 0.015, 0.048, and 0.091, respectively. The scattering intensity was normalized with respect to the scattering intensity of the lowest temperature point of each curve.

Deleted: <sp>

Deleted: average s

Deleted:

Deleted: pure DMPG samples at the lowest temperature

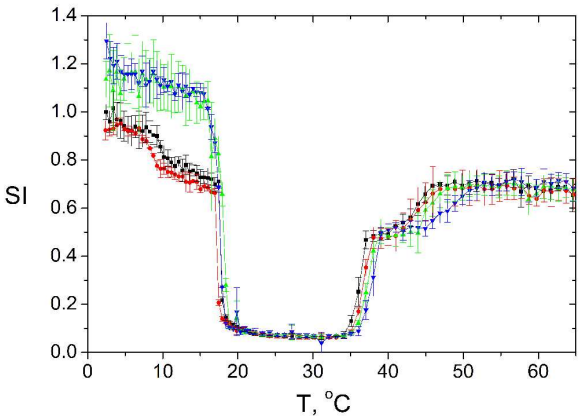

Supporting information figure 8. The 90° scattering intensities for C3S-PG-containing DMPG vesicles as a function of temperature. The black squares are the data in the absence of C3S, and the red circles, green up triangles, and blue down triangles, and orange stars represent data for X_{C3S} = 0.010, 0.024, and 0.048, respectively. The scattering intensity was normalized with respect to the average scattering intensity of pure DMPG samples at the lowest temperature.

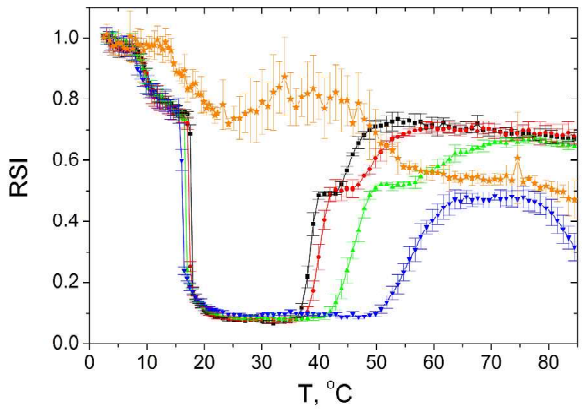

Supporting information figure 9. The relative 90° scattering intensities for lyso-PG-containing DMPG vesicles as a function of temperature. The black squares are the data in the absence of lyso-PG, and the red circles, green up triangles, blue down triangles, and orange stars represent data for $X_{lyso\text{-}PG}$ = 0.015, 0.048, 0.091, and 0.130, respectively. The scattering intensity was normalized with respect to the lowest temperature point of each curve.

Deleted: average scattering intensity of pure DMPG samples at the lowest temperature.

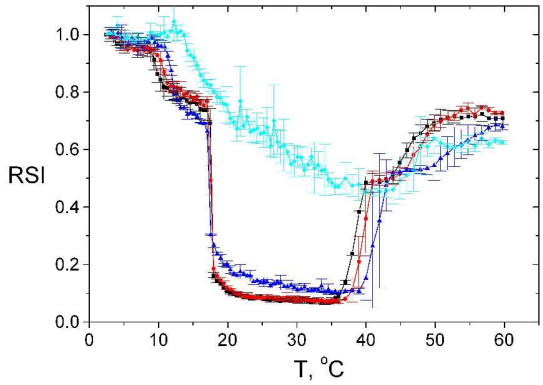

Supporting information figure 10. The 90° light scattering heating scans of 1 mM DMPG in the presence of 0, 0.5, 1.0, and 2.0 M urea (black squares, red circles, blue up triangles and cyan diamonds, respectively). The scans are normalized relative to scattering intensity at the first point of each curve.

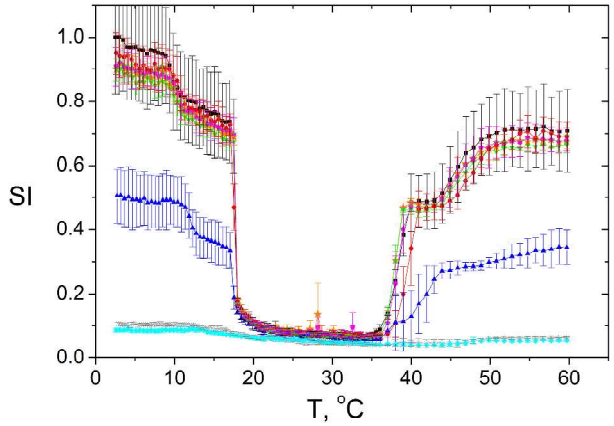

Supporting information figure 11. The 90° scattering intensities for DMPG vesicles in the presence of urea. The black squares are the data in the absence of urea, and the orange stars, green down triangles, magenta pentagons, red circles, blue up triangles, gray crosses, and cyan diamonds represent data for urea = 0.05, 0.10, 0.20, 0.50, 1.0, 1.5, and 2.0 M, respectively. The scattering intensity was normalized with respect to the average scattering intensity of pure DMPG samples at the lowest temperature.

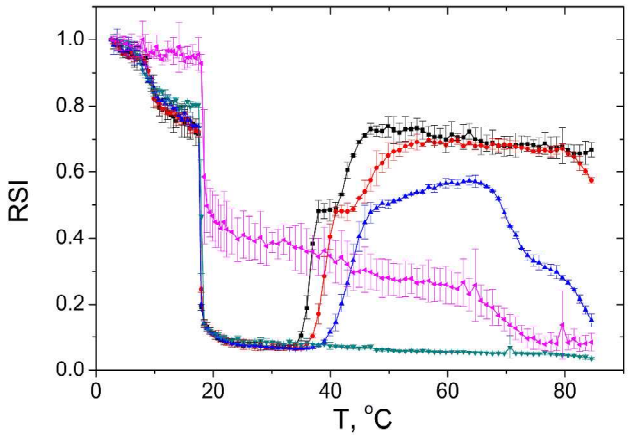

Supporting information figure 12. The 90° scattering intensities for DMPG vesicles in the presence of EtOH. The black squares are the data in the absence of EtOH, and the red circles, blue up triangles, dark cyan down triangles, and magenta diamonds for EtOH = 0.5, 1.0, 2.5, 5.0, and 10

vol%, respectively. The scattering intensity was normalized with respect to the scattering intensity of each curve at the lowest temperature.

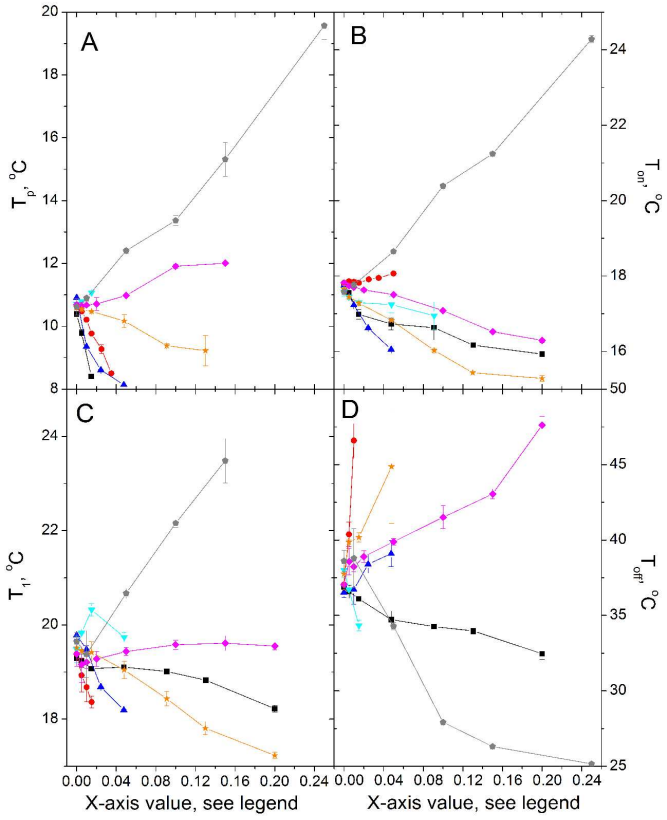

Supporting information figure 13. The transition temperatures from DSC data. In panels A, B, C, and D the transition temperatures T_p, T_{on}, T_1, and T_{off} are shown, respectively. The x-axis represent mole fraction in the bilayer for cholesterol, cholesterol-3-sulphate, dimyristoylglycerol, and lyso-PG. For ethanol and DMSO the x-axis represents the mixing volume fraction in the buffer. For urea the x-axis is the urea concentration in damol/l, i.e. value 0.2 represents urea concentration 2.0 mol/l. The data for CHOL (black squares), C3S (blue up triangles), DMG (cyan down triangles), lyso-PG

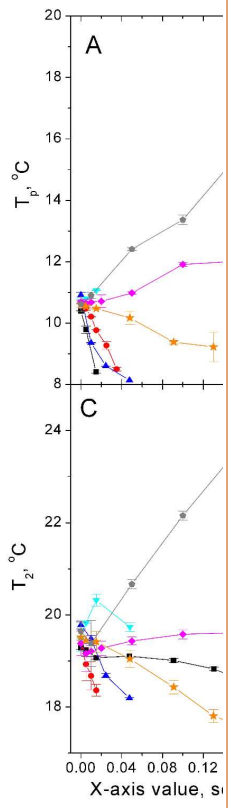

Deleted: average

Deleted: pure DMPG samples

Deleted:

Deleted: 1

Deleted: 2

Deleted: 4

(orange stars), EtOH (red circles), urea (magenta diamonds), and DMSO (gray pentagons) are shown.

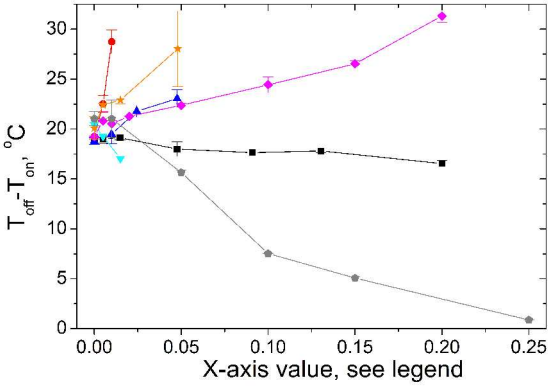

Supporting information figure 14. The temperature span of the intermediate state, T_{off}-T_{on}, as observed from the endotherms. The x-axis represents mole fraction in bilayer for cholesterol, cholesterol-3-sulphate, dimyristoylglycerol, and lyso-PG. For ethanol and DMSO the x-axis represents the mixing volume fraction in the buffer. For urea the x-axis is the urea concentration as damol/l, i.e. value 0.2 represents urea concentration 2.0 mol/l. The data for CHOL (black squares), C3S (blue up triangles), DMG (cyan down triangles), lyso-PG (orange stars), EtOH (red circles), urea (magenta diamonds), and DMSO (gray pentagons) are shown.

Deleted: T_4

Deleted: 1

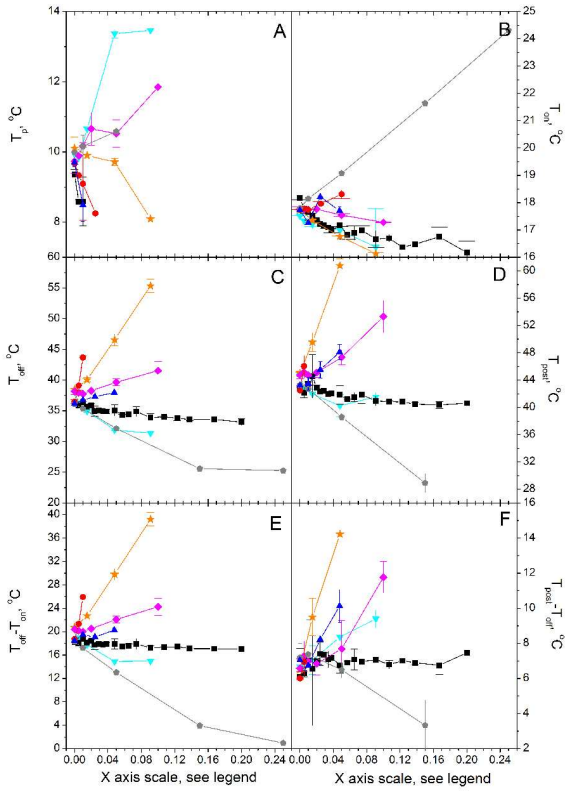

Supporting information figure 15. The transition temperatures from 90° light scattering data. The pretransition temperature (panel A), the temperature (T_{on}) for the appearance of intermediate state (panel B), the temperature (T_{off}) for the disappearance of intermediate state (panel C), the high temperature scattering only transition temperature T_{post} (panel D), and the temperature span of the intermediate state T_{off}-T_{on} (panel E) as well as the temperature difference between T_{post} and T_{off}, T_{post}-T_{off} (panel F). The x-axis represent mole fraction in bilayer for cholesterol, cholesterol-3-sulphate, dimyristoylglycerol, and lyso-PG. For ethanol and DMSO x-axis represents the mixing volume fraction in the buffer. For urea the x-axis is the urea concentration as damol/l, i.e. value 0.2 represents urea concentration 2.0 mol/l. The data for CHOL (black squares), C3S (blue up triangles), DMG (cyan down triangles), lyso-PG (orange stars), EtOH (red circles), urea (magenta diamonds), and DMSO (gray pentagons) are shown.

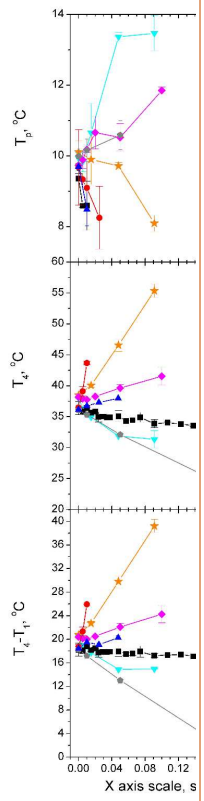

Deleted:

Deleted: 1

Deleted: T4

Deleted: 5

Deleted: T4

Deleted: T1

Deleted: 5

Deleted: T4

Formatted: Subscript

Deleted: 5

Deleted: T4

Deleted: Page Break

Section 2: Calculation of the area and volume in rims of the hole

For a hole with an angle θ between the lines going from the centre of a spherical vesicle to the center of the hole and the rim of the hole, the area and volume for the lipid in the hole rims are (as can be easily obtained by integration):

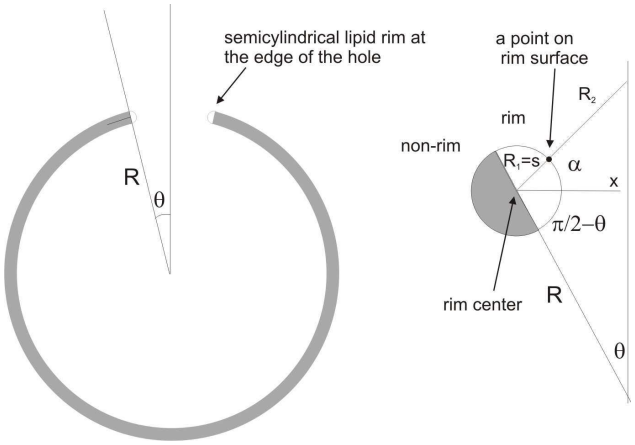

$$A_{rim} = 2\pi^2 Ra\sin\theta - 4\pi a^2\cos\theta$$

$$V_{rim} = \pi^2 Ra^2\sin\theta - \frac{4}{3}\pi a^3\cos\theta$$

where R is the apparent vesicle radius from the centre of the vesicle to the centre of the bilayer and a is the monolayer thickness.

Likewise, the area and volume of the bilayer in the vesicle without holes are

$$A_{sphere} = 4\pi\left(R^2 + a^2\right)$$

$$V_{sphere} = \frac{4\pi}{3}\left(6R^2a + 2a^3\right)$$

and the missing area and volume from the surface of the vesicle because the presence of a hole are:

$$A_{hole} = 2\pi\left(R^2 + a^2\right)\left(1-\cos\theta\right)$$

$$V_{hole} = \frac{2\pi}{3}\left(6R^2a + 2a^3\right)\left(1-\cos\theta\right)$$

Now, let us assume that initially we have a spherical vesicle with 70 nm radius without any holes. Then the area and the volume for the bilayer of this vesicle are approximately A_0=61600 nm^2 and V_0=277000 nm^3.

When we introduce *n* holes into this vesicle, then if the volume of the bilayer required to fill a hole is larger than the volume of the lipid in the rims of the hole, then the vesicle needs to expand (*R* increases) to accommodate the bilayer volume from the holes. Thus

$$V_0 = V_{sphere} - nV_{hole} + nV_{rim} = R^2\left\{4\pi a\left[2 - n\left(1 - \cos\theta\right)\right]\right\} + R\left\{\pi^2 a^2 n\cos\theta\right\} + \frac{4\pi}{3}a^3\left(2 - n\right).$$

We can now calculate the radius for the vesicle with holes utilizing the bilayer volume V_0.

$$R = \frac{-\pi^2 a^2 n\cos\theta + \sqrt{\left(\pi^2 a^2 n\cos\theta\right)^2 - 4\cdot\left\{4\pi a\left[2 - n\left(1 - \cos\theta\right)\right]\right\}\cdot\left[\frac{4\pi}{3}a^3\left(2 - n\right) - V_0\right]}}{2\cdot\left\{4\pi a\left[2 - n\left(1 - \cos\theta\right)\right]\right\}}.$$

Riske et al.[8] observed in their SAXS and WAXS measurement a repeat distance of 40 nm, suggesting that the largest hole diameter (for cage-like vesicle) cannot be larger than this. Let us assume that the maximum hole diameter

$d_{hole} = 2R\sin\theta = 40$ nm.

Now the hole angle and vesicle radius can be solved numerically for any number n of holes. We calculated the apparent vesicle radius, the fraction of the total lipid volume in the rims (=the fraction of lipid molecules in the rims), and the apparent volume fraction due to the enlargement of the particles.

Thus the apparent radius of the vesicle, the fraction of lipid volume (=the fraction of lipids) in the rims around the holes, and the relative change in apparent fraction of the total solution volume inside the holey vesicles can be then calculated.